Journal of Engineering Mathematics, Vol. 8, No. 4, October 1974
Noordhoff International Publishing – Leyden
Printed in The Netherlands

Numerical studies of steady, viscous incompressible flow in a quasi two-dimensional problem

R. A. MERIC

Applied Mathematics Division, The Scientific and Technical Research Council of Turkey, Marmara Scientific and Industrial Research Institute, Kocaeli, Turkey

N. A. MACKEN

Department of Mechanical Engineering, Carnegie-Mellon University, Pittsburgh, Pennsylvania, USA

(Received September 10, 1973 and in final form January 10, 1974)

SUMMARY
A quasi two-dimensional fluid flow problem, a channel with a cavity, is solved by finite-difference techniques. The numerical method used gives convergent results for all Reynolds numbers studied.

1. Introduction

When a fully developed assumption is made in one of the directions of an orthogonal coordinate system, the three-dimensional Navier–Stokes equations become quasi two-dimensional in steady, incompressible viscous flow. The flow exists in all three directions but there is no variation in the fully developed direction.

The numerical solution of the quasi two-dimensional Navier–Stokes equations is given below for the problem of flow in a channel with a rectangular cavity. This problem configuration is encountered, for example, in the parallel flat plate models of viscoseals [1]. The flow equations are solved by a finite-difference technique.

2. Formulation of the problem

Consider the parallel flat plate model of a viscoseal illustrated in Fig. 1. The flat plate with the grooves is taken as stationary while the smooth flat plate on top is moving with the velocity 1 in the x'-direction. The y–z cross section of the flow domain of one typical groove-ridge pair is

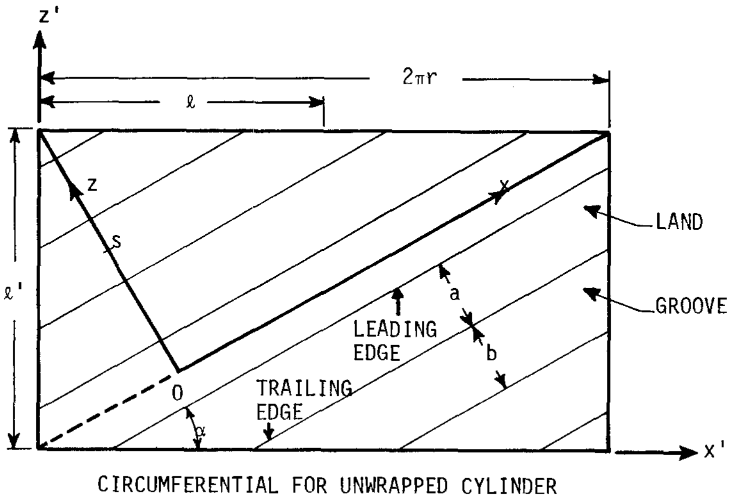

Figure 1. Plan view of mathematical model of parallel groove-ridge geometry.

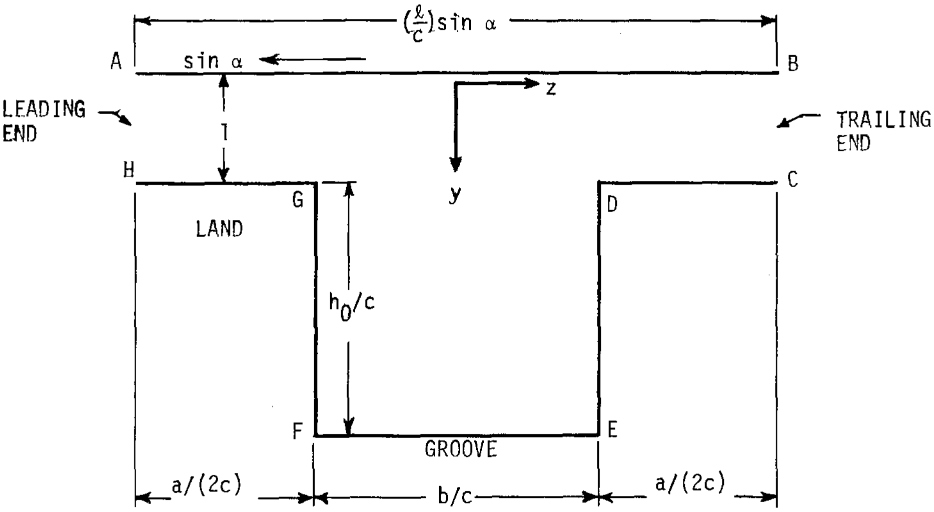

Figure 2. Cross-sectional view along z-axis of one-groove-ridge pair.

shown in Fig. 2. When the assumption that the flow is fully developed in the x-direction is introduced, the Navier–Stokes equations take the form

$$v\frac{\partial v}{\partial y} + w\frac{\partial v}{\partial z} = -\frac{\partial p}{\partial y} + \frac{1}{\mathrm{Re}}\left(\frac{\partial^2 v}{\partial y^2} + \frac{\partial^2 v}{\partial z^2}\right) \tag{1}$$

$$v\frac{\partial w}{\partial y} + w\frac{\partial w}{\partial z} = -\frac{\partial p}{\partial z} + \frac{1}{\mathrm{Re}}\left(\frac{\partial^2 w}{\partial y^2} + \frac{\partial^2 w}{\partial z^2}\right) \tag{2}$$

$$\frac{\partial v}{\partial y} + \frac{\partial w}{\partial z} = 0 \tag{3}$$

$$v\frac{\partial u}{\partial y} + w\frac{\partial u}{\partial z} = -\frac{\partial p}{\partial x} + \frac{1}{\mathrm{Re}}\left(\frac{\partial^2 u}{\partial y^2} + \frac{\partial^2 u}{\partial z^2}\right) \tag{4}$$

where $\partial p/\partial x =$ constant, u, v, w are the velocity components in the x, y, z-directions, p is the pressure, and Re is the Reynolds number.

Now, a two-dimensional stream function, $\psi(y, z)$, and vorticity function, $\xi(y, z)$, are defined by

$$w = \frac{\partial \psi}{\partial y}, \quad v = -\frac{\partial \psi}{\partial z}, \tag{5a}$$

and

$$\xi = \frac{\partial w}{\partial y} - \frac{\partial v}{\partial z}. \tag{5b}$$

Introducing the new variables into equations (1) through (3) we have

$$\frac{\partial^2 \xi}{\partial y^2} + \frac{\partial^2 \xi}{\partial z^2} + \mathrm{Re}\left(\frac{\partial \psi}{\partial z}\frac{\partial \xi}{\partial y} - \frac{\partial \psi}{\partial y}\frac{\partial \xi}{\partial z}\right) = 0 \tag{6}$$

where

$$\xi = \frac{\partial^2 \psi}{\partial y^2} + \frac{\partial^2 \psi}{\partial z^2}. \tag{7}$$

The quasi two-dimensional flow problem, therefore, is described by equations (4), (6), and (7). Equations (6) and (7) are referred to as the vorticity (transport) equation, and the stream function equation, respectively.

Equations (6) and (7) can be solved for the y–z flow field in terms of the functions ψ and ξ. The boundary conditions to be satisfied are (refer to Fig. 2)

$$\psi = \psi_Q, \ \frac{\partial\psi}{\partial y} = -\sin\alpha, \text{ on } \overline{AB}; \tag{8}$$

$$\psi = 0, \ \frac{\partial\psi}{\partial y} = 0, \qquad \text{on } \overline{CD}, \overline{EF}, \overline{GH}\ ; \tag{9}$$

$$\psi = 0, \ \frac{\partial\psi}{\partial z} = 0, \qquad \text{on } \overline{DE}, \overline{FG}\,, \tag{10}$$

where ψ_Q is the guess value of the stream function on the smooth flat plate, and α is the angle between the x- and x'-directions. Since the flow fields are similar in different groove-land pairs the periodicity conditions exist on $\overline{BC}$ and $\overline{AH}$, i.e.,

$$\psi[y, -l\sin\alpha/(2c)] = \psi[y, l\sin\alpha/(2c)] \tag{11}$$

$$\xi\,[y, -l\sin\alpha/(2c)] = \xi\,[y, l\sin, \alpha/(2c)] \tag{12}$$

$$\frac{\partial^{n+m}\psi[y, -l\sin\alpha/(2c)]}{\partial y^n\partial z^m} = \frac{\partial^{n+m}\psi[y, l\sin\alpha/(2c)]}{\partial y^n\partial z^m} \tag{13}$$

$$\frac{\partial^{n+m}\xi\,[y, -l\sin\alpha/(2c)]}{\partial y^n\partial z^m} = \frac{\partial^{n+m}\xi\,[y, l\sin\alpha/(2c)]}{\partial y^n\partial z^m} \tag{14}$$

for $0 \leqq n, m \leqq \infty$.

The vorticity, ξ, does not have explicit boundary values. The ξ-boundary values are corrected for initial guesses as the y–z flow field is being solved.

Before attacking the x-momentum equation (4), it is necessary to calculate for the pressure gradient in the x-direction. For a cylindrical viscoseal geometry, $\partial p/\partial x$ is given by [1]

$$\frac{\partial p}{\partial x} = \frac{N(\Delta p_{r+g})_z}{2\pi r\cos\alpha} \tag{15}$$

where N is the number of helix starts, r is the rotor radius, and $(\Delta p_{r+g})_z$ is the pressure difference between the leading and trailing ends of a groove-ridge pair cross section (Fig. 2). After solving equations (6) and (7), the value of $(\Delta p_{r+g})_z$ can be found from the integrated form of the z-momentum equation, i.e.,

$$(\Delta p_{r+g})_z = \frac{1}{2}\left(q_1^2 - q_2^2\right) + \frac{1}{\text{Re}}\int_1^2 \frac{\partial\xi}{\partial y}\,dz - \int_1^2 v\xi\,dz \tag{16}$$

where $q^2 = v^2 + w^2$, and the point 1 corresponds to $z = -l\sin\alpha/(2c)$, and the point 2 to $z = l\sin\alpha/(2c)$.

Now, the x-momentum equation (4), after introducing the stream function gradients for the velocities v and w, and using the calculated value of $\partial p/\partial x$, can be solved for the velocity u. The u-velocity boundary conditions are

$$u = \cos\alpha, \text{ on } \overline{AB}; \tag{17}$$

$$u = 0, \qquad \text{on } \overline{CD}, \overline{DE}, \overline{EF}, \overline{FG}, \overline{GH}\,. \tag{18}$$

On $\overline{BC}$ and $\overline{AH}$ the periodicity conditions prevail, i.e.,

$$u[y, -l\sin\alpha/(2c)] = u[y, l\sin\alpha/(2c)] \tag{19}$$

$$\frac{\partial^{n+m}u[y, -l\sin\alpha/(2c)]}{\partial y^n\partial z^m} = \frac{\partial^{n+m}u[y, l\sin\alpha/(2c)]}{\partial y^n\partial z^m}\,. \tag{20}$$

After solving the x-momentum equation, the net volume flow rate, Q_{ax}, in the z'-direction is checked to see if the condition $Q_{ax}=0$ has been reached with the guessed value of ψ_Q. The volume flow rate Q_{ax} can be found from

$$Q_{ax}=\int_0^{l/c}\int_0^{h(x')}u(y,x')\sin\alpha dydx'+\frac{l}{c}\int_0^1 w(y,x')\cos\alpha dy \tag{21}$$

where $h(x')$ is the nondimensional distance from the smooth plate to the grooved plate as a function of x'.

3. The numerical method

The vorticity transport equation (6), the stream function equation (7), and x-momentum equation (4) are solved by finite-difference techniques. In order to represent the equations by finite-difference forms, a nonuniform rectilinear mesh is superimposed over the y–z domain. Mesh sizes Δy's, and Δz's are taken relatively small next to the boundaries for accuracy.

First the coupled vorticity equation (6) and the stream function equation (7) are solved simultaneously. At the interior and boundary grid points, a pair of finite sequences of discrete functions are constructed as follows:

$$\psi^{(0)},\psi^{(1)},\psi^{(2)},\dots,\psi^{(n-1)},\psi^{(n)} \tag{22}$$

$$\xi^{(0)},\xi^{(1)},\xi^{(2)},\dots,\xi^{(n-1)},\xi^{(n)} \tag{23}$$

For given tolerance ε_ψ and ε_ξ

$$|\psi^{(n)}-\psi^{(n-1)}|\leqq\varepsilon_\psi,\ |\varepsilon^{(n)}-\xi^{(n-1)}|\leqq\varepsilon_\xi \tag{24}$$

at each grid point of the domain.

At each grid point on $\overline{AB}$, $\psi^{(0)}$ is taken as ψ_Q; a guess value which is iterated for $Q_{ax}=0$. On $\overline{CD}$, $\overline{DE}$, $\overline{EF}$, $\overline{FG}$, and $\overline{GH}$ the value of $\psi^{(0)}$ is set to zero. The initial guess for the remaining discrete stream function values is determined by linear interpolation along the vertical grid lines of the polygon ABCDEFGH (see Fig. 2). At each grid point the value of $\xi^{(0)}$ is set to zero.

The second element of sequence (22) is now determined as follows. On $\overline{AB}$, for each grid point set $\psi^{(1)}=\psi_Q$; at each grid point on CDEFGH set $\psi^{(1)}=0$. To find $\psi^{(1)}$ of the remaining grid points, the stream function equation (7), and the periodicity conditions (11) and (13) are written for each point in a finite-difference form by using central differences. The resulting linear algebraic system is then solved by successive overrelaxation and the solution is denoted by $\bar{\psi}^{(1)}$. The function $\psi^{(1)}$ is then defined by the weighed average

$$\psi^{(1)}=\rho_\psi\psi^{(0)}+(1-\rho_\psi)\bar{\psi}^{(1)},\qquad 0\leqq\rho_\psi\leqq 1\,. \tag{25}$$

After completely defining $\psi^{(1)}$ at each grid point of ABCDEFGH, the second element of sequence (23) is now determined. With the set of values of $\psi^{(1)}$, the boundary grid point values of the vorticity are corrected by a second order approximation. The stream function is expanded about two points next to the boundary under consideration in a Taylor series, and the appropriate value of the velocity is substituted for the first derivatives of the stream function. The corrected values of $\bar{\xi}^{(1)}$ at the boundary grid points are weight averaged by μ such that

$$\xi^{(1)}=\mu\xi^{(0)}+(1-\mu)\bar{\xi}^{(1)},\qquad 0\leqq\mu\leqq 1 \tag{26}$$

defining the new set of values $\xi^{(1)}$ for those points.

To find $\xi^{(1)}$ for the interior points, the vorticity equation (6) is approximated by a finite-difference form as follows. The second derivatives of the vorticity, ξ, and the first derivatives of the stream function, ψ, are replaced by "second order" central differences. The first order derivatives of the vorticity, ξ, are approximated by backward or forward differences depending on whether the coefficients of these derivatives are positive or negative [2]. This method yields diagonally dominant systems of linear algebraic equations for all Reynolds numbers, Re. The generated algebraic equations are then solved by successive underrelaxation, and the solution is denoted by $\bar{\xi}^{(1)}$ of the interior grid points. The function $\xi^{(1)}$ is then determined at the interior points by the weighted average

$$\xi^{(1)} = \rho_\xi \xi^{(0)} + (1-\rho_\xi)\bar{\xi}^{(1)}, \qquad 0 \leqq \rho_\xi \leqq 1 \,. \tag{27}$$

The numerical method is repeated for the other elements of sequences (22) and (23) until, for some n, (24) is valid. The final elements $\psi^{(n)}$ and $\xi^{(n)}$ will constitute the solution to the difference approximations of equations (6) and (7) for a guess value of ψ_Q.

The pressure difference between $\overline{BC}$ and $\overline{AH}$ at y = constant is numerically found from equation (16) by using Simpson's 1/3 and 3/8 rules. Then, $\partial p/\partial x$ is calculated by means of equation (15).

Now, the u-velocity equation (4) is put in a finite-difference form. The first order derivatives of u are expressed by backward or forward differences depending on whether the coefficients of these derivatives are positive or negative. The other derivatives are approximated by central differences. Then, the discrete u-velocity values on and within the polygon ABCDEFGH are found by successive overrelaxation.

Knowing all the discrete velocity values for the y–z domain, the volume flow rate, Q_{ax}, is calculated from equation (21) using Simpson's rules. The whole numerical procedure is repeated if the desired value of Q_{ax} has not been reached with the guess value of ψ_Q.

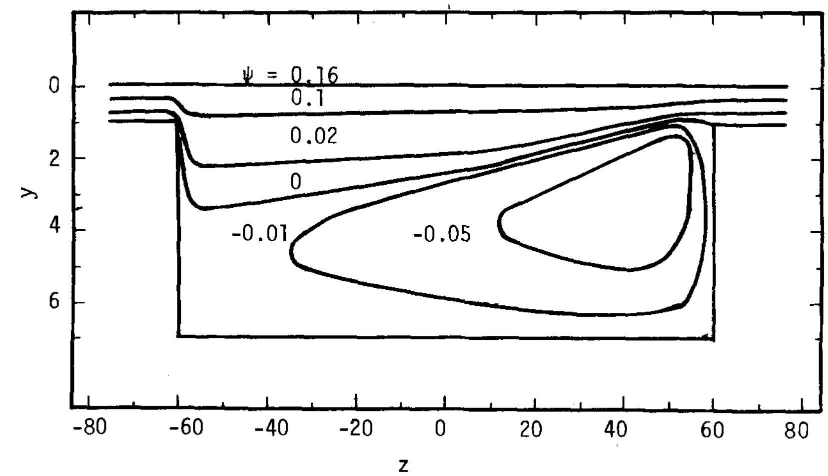

Figure 3. Constant stream function curves at Re = 300 of geometry $a/c=32$, $b/c=120$, $h_0/c=6$, $\alpha=6°$, $N=1$.

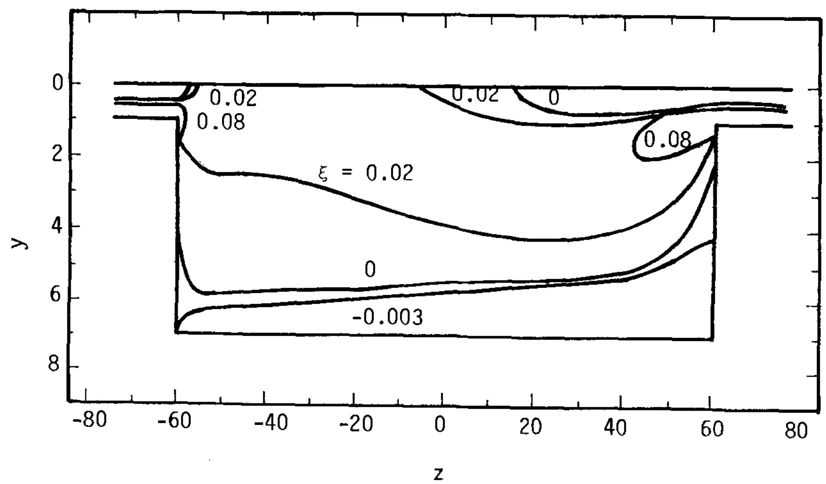

Figure 4. Constant vorticity curves at Re = 300 of geometry $a/c=32$, $b/c=120$, $h_0/c=6$, $\alpha=6°$, $N=1$.

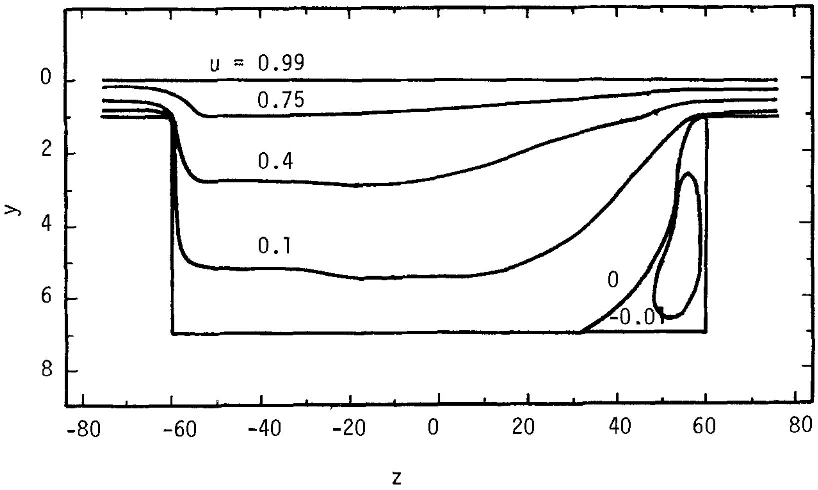

Figure 5. Constant u-velocity curves at $Re=300$ of geometry $a/c=32$, $b/c=120$, $h_0/c=6$, $\alpha=6^\circ$, $N=1$.

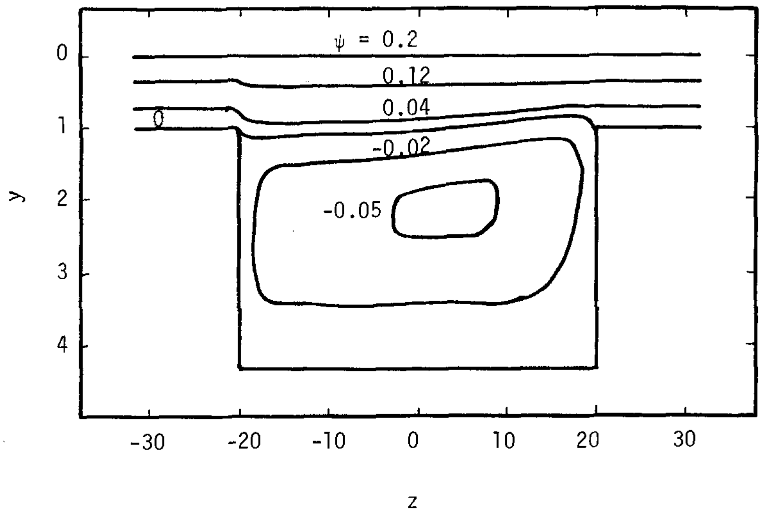

Figure 6. Constant stream function curves at $Re=300$ of geometry $a/c=25$, $b/c=41$, $h_0/c=3.4$, $\alpha=10^\circ$, $N=8$.

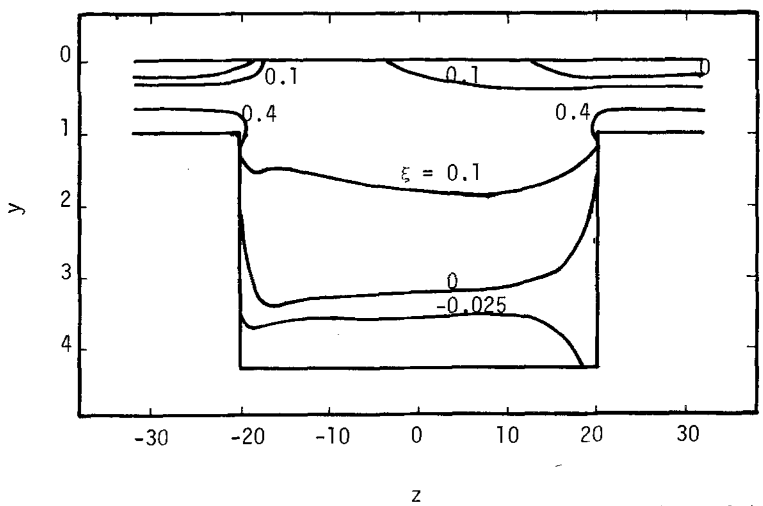

Figure 7. Constant vorticity curves at $Re=300$ of geometry $a/c=25$, $b/c=41$, $h_0/c=3.4$, $\alpha=10^\circ$, $N=8$.

4. Examples

The numerical procedure was tested with several geometries. The mesh distribution, relaxation and weighted averaging parameters depended on the geometry considered and the Reynolds number. Convergent results were obtained readily for $\varepsilon_\psi = 10^{-6}$, $\varepsilon_\xi = 10^{-6}$, $\rho_\psi = 0.05$, $\mu = 0.05$, and $\rho_\xi = 0.7$ even for high Reynolds numbers on the Univac 1108 computer system. A variety of checks were made to determine the validity of the results. In a given special case the numerical method yielded essentially the same result as an analytical method.

Numerical results for different geometries are shown in Figures 3 through 9. The presented curves were generated by simple linear interpolation for constant value of the variables. The streamline contours for the y–z flow field shown in Fig. 3,6, and 9 are in qualitative agreement with those of similar flow field problems analyzed by other authors [2· 3, 4, 5]. The presented solutions for the flow problem corresponded to $Q_{ax} = 0$.

5. Conclusions

The numerical method presented here is straightforward, and convergent for all Reynolds num-

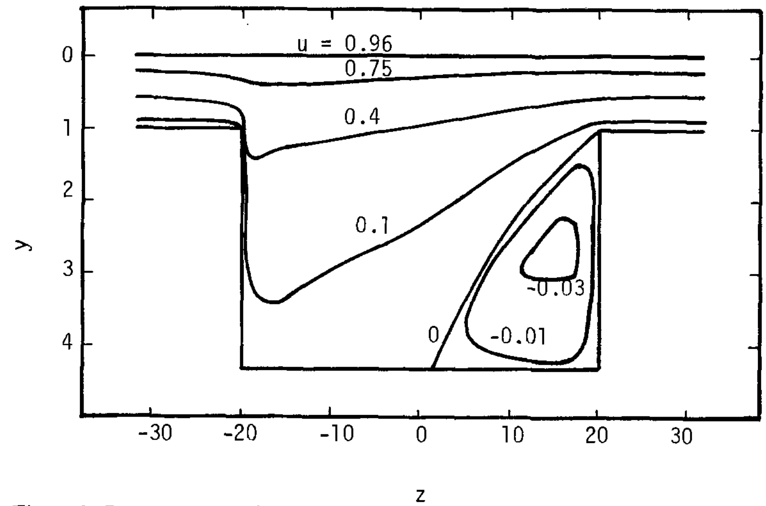

Figure 8. Constant u-velocity curves at Re = 300 of geometry $a/c = 25$, $h/c = 41$, $h_0/c = 3.4$, $\alpha = 10°$, $N = 8$.

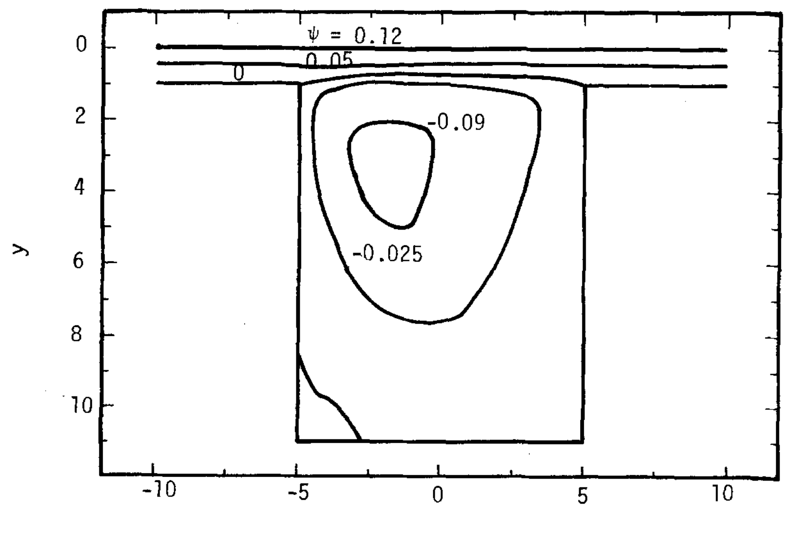

Figure 9. Constant stream function curves at Re = 300 of geometry $a/c = 10$, $b/c = 10$, $h_0/c = 10$, $\alpha = 10°$, $N = 4$.

bers studied. However, as expected, the convergence rate depends on the geometry of the domain and also on the Reynolds number. The method is general, and can be applied to solve any quasi two-dimensional problem.

Acknowledgment

This work was supported by the National Science Foundation Grant No. GK27831.

REFERENCES

[1] R. A. Meric, *Convective Inertia Effects in the Viscoseal*, Ph.D. Thesis, Carnegie-Mellon University (1973).
[2] D. Greenspan, Numerical Studies of Steady, Viscous, Incompressible Flow in a Channel with a Step, *Journal of Engineering Mathematics*, 3 (1969) 21–28.
[3] M. Kawaguti, *Numerical Solution of the Navier–Stokes Equations for Flow in a Channel with a Step*, MRC-TSR-574, University of Wisconsin (1965).
[4] U. B. Mehta and Z. Lavan, *Flow in a Two-Dimensional Channel with a Rrectangular Cavity*, NASA CR-1245 (1969).
[5] H. A. Putre, *Computer Solution of Unsteady Navier–Stokes Equations for an Infinite Hydrodynamic Step Bearing*, NASA TN D-5882 (1970).